Diffusive Dynamics of Charge Regulated Macro-ion Solutions

Bin Zheng,[1] Shigeyuki Komura,[1,2,3] David Andelman,[4,5] and Rudolf Podgornik[6,1,7,a)]

[1)] *Wenzhou Institute, University of Chinese Academy of Sciences, Wenzhou, Zhejiang 325001, China*

[2)] *Oujiang Laboratory, Wenzhou, Zhejiang 325000, China*

[3)] *Department of Chemistry, Graduate School of Science, Tokyo Metropolitan University, Tokyo 192-0397, Japan*

[4)] *School of Physics and Astronomy, Tel Aviv University, Ramat Aviv 6997801, Tel Aviv, Israel*

[5)] *Center of Physics and Chemistry of Living Systems, Tel Aviv University, Ramat Aviv 6997801, Tel Aviv, Israel*

[6)] *School of Physical Sciences and Kavli Institute for Theoretical Sciences, University of Chinese Academy of Sciences, Beijing 100049, China*

[7)] *CAS Key Laboratory of Soft Matter Physics, Institute of Physics, Chinese Academy of Sciences, Beijing 100190, China*

(*Electronic mail: podgornikrudolf@ucas.ac.cn.)

(*Electronic mail: andelman@post.tau.ac.il)

(*Electronic mail: komura@wiucas.ac.cn)

(*Electronic mail: zhengbin@ucas.ac.cn)

(Dated: 26 April 2025)

Onsager's variational principle is generalized to address the diffusive dynamics of an electrolyte solution composed of charge-regulated macro-ions and counterions. The free energy entering the Rayleighian corresponds to the Poisson-Boltzmann theory augmented by the charge-regulation mechanism. The dynamical equations obtained by minimizing the Rayleighian include the classical Poisson-Nernst-Planck equations, the Debye-Falkenhagen equation, and their modifications in the presence of charge regulation. By analyzing the steady state, we show that the charge regulation impacts the non-equilibrium macro-ion spatial distribution and their effective charge, deviating significantly from their equilibrium values. Our model, based on Onsager's variational principle offers a unified approach to the diffusive dynamics of electrolytes containing components that undergo various charge association/dissociation processes.

Charged macro-ions in solution do not keep their charge fixed but rather respond to the local environment by modifying their surface charge density and surface potential, depending on their local concentration and the bathing solution conditions[1–3]. This conceptual framework is called *charge regulation* (CR), encompassing charging equilibria of macromolecules in ionic solutions. It is ubiquitous and governs important aspects of electrostatic interactions in biological systems[4,5].

The CR phenomenon is essential in understanding how proteins and charged biomolecules change their state via charge association/dissociation processes[6] involving ions in solutions[7]. In particular, it affects polyelectrolytes that undergo protonation/deprotonation reactions on acidic/basic sites[8,9], protein complexation[10], polyelectrolyte gel swelling[11], adsorption of charge particles onto surfaces[12,13], bacterial adhesion[14], viral capsids assembly[15], zwitterionic colloids and nanoparticles[16,17], as well as many other bio-processes.

Equilibrium CR effects have been extensively studied by including the association/dissociation equilibrium into the mean-field Poisson-Boltzmann (PB) theory[3]. However, despite the large progress in the study of equilibrium CR phenomena[3], starting from the seminal work of Ninham and Parsegian[18], a theoretical understanding of *dynamical* CR behavior is less developed. Nevertheless, the latter has pronounced importance in numerous physical and chemical processes, such as the kinetics of surfactant adsorption at the air/water interface[19,20], interactions and dynamics of polyelectrolytes, gels, and colloids[21–23], and ionic conductance through nano-tubes[24] and nano-channels[25,26].

Conventional theoretical studies of charged macro-ion dynamics driven by external electric fields are typically based on the Poisson-Nernst-Planck (PNP) theory[27]. This theory is a diffusive kinetic extension of the PB formulation of electrostatics. It has been generalized to include ion-ion interactions and steric effects[28]. However, a complete theory of CR dynamics would need even further modifications. It should include a description of the charge dissociation processes[21,29,30], either on the system bounding surfaces[31] or on the surface of the mobile macro-ions[32] containing the dissociable moieties. In order to formulate these ideas into a consistent theoretical description, we select the framework outlined by Onsagers variational principle (OVP)[33–35]. The OVP provides an elegant foundation for addressing non-equilibrium processes in soft matter systems. It is a useful framework because it offers significant flexibility in choosing appropriate pairs of state variables and velocities based on Rayleigh's principle of least energy dissipation. This crucial aspect tackles the main challenges in formulating kinetic descriptions of Onsagers theory and deriving thermodynamically consistent dynamical equa-

[a)] Deceased, Dec. 28, 2024.

tions. Consequently, many established kinetic equations describing various soft matter systems can be systematically derived within this framework[36–38].

OVP allows us to combine the CR theory already studied in thermodynamic equilibrium[3] with the non-equilibrium dissipation phenomenology, as represented by diffusion currents[39], charge currents[40] and chemical reaction kinetics[41]. By generalizing OVP even further and including the CR equilibrium free energy and its corresponding diffusive-current densities, we derive the Rayleighian that contains the CR diffusive components. Furthermore, our augmented theory yields a set of diffusive dynamic equations. They reduce, in the limit of fixed ionic charge, to the PNP[21,42] and Debye-Falkenhagen[43] equations. We explicitly solve these modified PNP diffusive-dynamic equations in the steady-state limit[44] and show that the CR significantly influences the spatial distribution and charge density in externally driven systems. There is a clear advantage in formulating the CR dynamics based on OVP. It presents a universal approach for deriving the CR diffusive dynamics directly from the equilibrium free energy while making it applicable to various CR models with potential implications for biological systems.

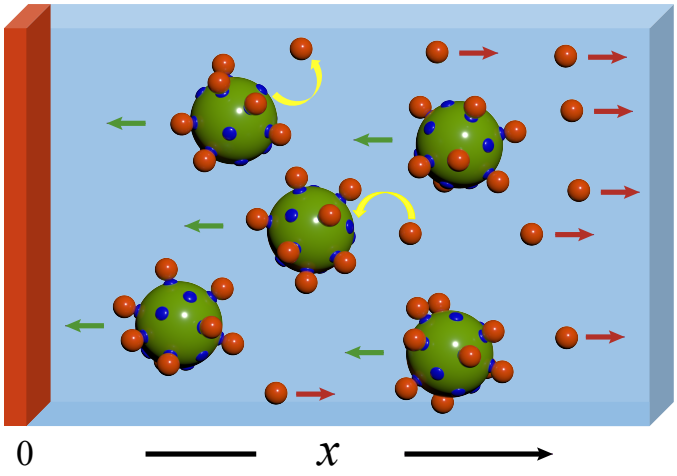

FIG. 1. Schematic presentation of our CR diffusive dynamical model. A positively charged wall (red) induces an external electric field, and is placed in contact with a semi-infinite ionic solution. The solution contains negatively charged macro-ions (green) and monovalent positive counter-ions (B^+, red) of bulk concentration n_b and p_b, respectively. Each CR macro-ion contains N negatively charged sites (A^-, blue). However, due to the association/dissociation process, the effective macro-ion charge can vary from $-Ne$ to zero. The yellow semicircular arrow corresponds to the association/dissociation reaction in Eq. (1).

We consider a positively charged planar boundary placed at $x = 0$. This plane induces a static electric field on a semi-infinite ionic solution, as shown in Fig. 1. The solution is composed of negatively charged macro-ions of spatially varying concentration $n(\mathbf{r})$ and bulk value n_b, and positively charged counter-ions concentration $p(\mathbf{r})$ of bulk value p_b (denoted as B^+). Each macro-ion contains N negatively charged sites (denoted as A^-), and each of the A^- sites can change its charge by an association/dissociation process,

$$A^- + B^+ \rightleftharpoons AB \tag{1}$$

The dynamical number fraction of A^- sites that are neutralized by B^+ is $\phi(\mathbf{r})$ and it varies from zero (when the macro-ions are fully charged) to unity (when the macro-ions are completely neutral).

In our model, the overall electro-neutral solution has no co-ions. This requires that the integrated number of A^- sites is equal to that of B^+. The electro-neutrality condition in bulk can be expressed as $p_b = n_b N(1-\phi_b)$, where ϕ_b is the equilibrated number fraction of neutralized A^- sites in the bulk.

Within the mean-field framework, the thermodynamic free energy F is a sum of the electrostatic free energy, the mobile ion translational entropy term $TS(p,n)$, and the CR free energy per macro-ion $g(\phi)$. Hence, F can be written as[29,32]

$$\begin{aligned} F[\psi,p,n,\phi] &= \int f(\psi,p,n,\phi)\,\mathrm{d}^3 r \\ &= \int \Bigg(-\frac{\varepsilon}{2}(\nabla\psi)^2 + e\psi\,[p - nN(1-\phi)] \\ &\quad + TS(p,n) + ng(\phi) \Bigg) \mathrm{d}^3 r, \end{aligned} \tag{2}$$

where $\psi(\mathbf{r})$ is the electrostatic potential, T is the temperature, $\varepsilon = \varepsilon_0 \varepsilon_r$ is the dielectric constant of the solution, ε_0 is the vacuum permittivity, ε_r is the relative permittivity, and e is the elementary charge. Furthermore,

$$S(p,n) = k_B \Big(p\left[\ln\left(pa^3\right) - 1\right] + n\left[\ln\left(na^3\right) - 1\right] \Big) \tag{3}$$

is the mixing entropy of counter-ions and macro-ions in the dilute solution limit, and k_B is the Boltzmann constant. For simplicity, the molecular size difference is ignored, and both macro-ions and counter-ions are assumed to have the same molecular volume, a^3.

To describe the charge association and dissociation processes governed by Eq. (1), we utilize the standard Langmuir isotherm. Although one can pursue a conventional kinetic derivation[2] starting from Eq. (1), it is more straightforward to employ an equivalent mean-field formalism based on the CR free energy[31,32], from which the Langmuir isotherm naturally arises through its minimization. Within this framework, ϕ is an annealed variable whose equilibrium value is determined by free energy minimization. The CR free-energy density $g(\phi)$ is given by

$$g(\phi) = N\Big(\alpha\phi + k_B T\left[\phi\ln\phi + (1-\phi)\ln(1-\phi)\right] \Big), \tag{4}$$

where α is the association/dissociation parameter, the last two terms correspond to the mixing entropy of N adsorption sites on each macro-ion. We note that generalized CR processes (beyond the Langmuir isotherm)[7,30], can be incorporated into our formalism[31]. For example, CR processes can

entail short-range interactions between adjacent charged adsorption sites[11,29].

Minimization of the free energy F with respect to ψ leads to the Poisson equation

$$\nabla^2\psi = -\frac{e}{\varepsilon}\left[p - nN(1-\phi)\right], \tag{5}$$

while the minimization with respect to the other variables p, n and ϕ yields the respective chemical potentials. Such thermodynamic equilibrium equations for a variant of the above model have already been investigated in Ref.[32] and will not be presented explicitly here.

Our system contains negatively charged macro-ions in one of the $i = 0, ..., N$ charge states, each with a number density n_i, and counter-ions of density p, where all sites on the macro-ion surface are assumed to be identical, with no interactions between them. The velocity of each macro-ion $\mathbf{v}_i$ with magnitude $v_i = |\mathbf{v}_i|$ depends on its charge state. Therefore, there are $N+1$ possible velocities fields of the macro-ions, and the velocity of the counter-ions is denoted as $\mathbf{v}_p$. The dissipation function Φ stems from the friction in the diffusive motion, as the mobile ions migrate with their respective velocities through the solvent. It is given as

$$\Phi = \frac{1}{2}\int\left[\sum_{i=0}^{N} n_i\xi_i v_i^2 \;+\; p\,\xi_p v_p^2\right]\mathrm{d}^3 r. \tag{6}$$

where $\{\xi_i\}$ and ξ_p are the corresponding $N+2$ *friction coefficients*.

In the spirit of the mean-field equilibrium theory, we proceed to simplify the above Φ by the following assumptions: (i) the macro-ions in any charge state are moving with the same average velocity $v_i = v$, where v relates to the macroscopic transport under the external field. (ii) Their friction coefficient is proportional to the number of B^+ absorbed ions. This assumption arises from a hydrodynamic consideration: a spherical particle moving in a viscous fluid exhibits a friction coefficient proportional to its size. This proportionality validates the linear size dependence $\xi_i = N\xi_s + i\,\xi_w$, $i = 0, ..., N$, where $N\xi_s$ the macro-ion's friction coefficient has no absorbed counter-ions and $i\,\xi_w$ is the added friction for the i-th charge state. It indicates that macro-ions' friction coefficient in different charge states results from the macro-ions bare friction coefficient and an additional increment dependent on adsorption, which is proportional to the number of absorbed counter-ions. Note that $\sum_{i=0}^{N} n_i = n$ as n is the total density of the macro-ions. In addition, on the mean-field level, we replace $\sum_{i=0}^{N} i\,n_i$ by an average over all the $\{i\}$ charge states $n\langle i\rangle = nN\phi = w$, where $w = s\phi$ and $s = nN$. Also, recall that ϕ is the number fraction of neutralized sites on the macro-ion. Then, Eq. (6) can be simplified and becomes

$$\Phi = \frac{1}{2}\int\left(s\xi_s v^2 + w\xi_w v^2 + p\,\xi_p v_p^2\right)\mathrm{d}^3 r. \tag{7}$$

On the mean-field level, the above equation implies that it is equivalent to consider that the dissipation comes from three types of mobile components: macro-ions that have no B^+ association with site density $s = Nn$, macro-ions with an average of $N\phi$ associated B^+ counter-ions and density $w = Nn\phi = s\phi$, and free positive counter-ions of density p. The velocities of the first two mobile components can, in principle, be defined as v_s and v_w, respectively. Still, for simplicity and clarity, we assume the same average velocity v for macro-ions in different charge states and a different velocity v_p for free mobile counter-ions in the limit of weakly charged macro-ions and dilute solution.

It is more convenient to express the free energy F, Eq. (2), as $F[\psi, s, w, p]$. We now write down the Rayleighian for the three mobile components and employ the Onsager's variational principle (OVP) to derive the dynamical equations[34,35]. The dissipation function can now be rewritten in terms of the respective *particle current densities* for each mobile component. In terms of the currents defined by $j_s = sv_s$, $j_w = wv_w$ and $j_p = pv_p$, we have

$$\Phi = \frac{1}{2\zeta}\int\left[\frac{j_s^2}{s} + \frac{j_w^2}{w} + \frac{j_p^2}{p}\right]\mathrm{d}^3 r, \tag{8}$$

where ζ is the mobility coefficient, and all three friction coefficients are assumed to be equal, $\xi_s{=}\xi_w{=}\xi_p{=}1/\zeta$. Finally, the Rayleighian, $R = \Phi + \partial_t F$, is composed of the dissipation function Φ plus the temporal free energy rate $\partial_t F = \partial F/\partial t$, and R is written as

$$\begin{aligned} R &= \Phi + \partial_t F \\ &= \Phi + \int\left[\frac{\partial f}{\partial\psi}\frac{\partial\psi}{\partial t} + \frac{\partial f}{\partial s}\frac{\partial s}{\partial t} + \frac{\partial f}{\partial w}\frac{\partial w}{\partial t} + \frac{\partial f}{\partial p}\frac{\partial p}{\partial t}\right]\mathrm{d}^3 r. \end{aligned} \tag{9}$$

We assume that the electrostatic potential ψ is a fast dynamical variable, as it responds much faster than the diffusion of the macro-ion. The characteristic time scale is related to the build-up of a diffusive double layer (the Debye relaxation time) $\tau_\mathrm{D} = \lambda_\mathrm{D}^2/D$, where λ_D (the Debye length) is about 1nm, and D (the diffusion constant) is about $10^{-9}\mathrm{m}^2/\mathrm{s}$. Clearly, as τ_D is on the order of nanoseconds, it is much faster than the typical dynamic diffusion timescale for macro-ions, which is in the order of milliseconds. This assumption justifies the validity of the Poisson equation, Eq. (5), $\delta F/\delta\psi = 0$. We further assume that the continuity relations always hold for the density variables s, w, and p. They connect the time derivative with the divergence of the respective current density,

$$\partial_t k = -\nabla\cdot\mathbf{j}_k \qquad \text{for} \qquad k = s, w, p. \tag{10}$$

Thus, the terms in the volume integral of the Rayleighian R in Eq. (9) can be transformed into purely spatial derivatives. The variation of R with respect to the current density variables, $\delta R/\delta j_k = 0$ then yields,

$$\begin{aligned} \mathbf{j}_s &= -\zeta\left[-es\nabla\psi + k_\mathrm{B}T\nabla n - \frac{k_\mathrm{B}Ts}{1-w/s}\nabla\left(\frac{w}{s}\right)\right], \\ \mathbf{j}_w &= -\zeta\left[ew\nabla\psi + \frac{k_\mathrm{B}Ts}{1-w/s}\nabla\left(\frac{w}{s}\right)\right], \\ \mathbf{j}_p &= -\zeta\left[ep\nabla\psi + k_\mathrm{B}T\nabla p\right]. \end{aligned} \tag{11}$$

Note that the CR parameter α does not appear in the ionic currents as detailed in the above equations. This is because the CR parameter α lacks spatial dependence, resulting in a zero gradient in the term $\nabla(\delta g(\phi)/\delta\phi)$. However, α still determines the equilibrated number fraction of neutralized A^+ sites and influences the CR strength. Currents of more general CR models[11,29], can be derived within the OVP framework and will explicitly include the CR parameter.

A few special cases derived from Eq. (11) are of interest. In thermodynamic equilibrium, the time derivatives in Eq. (10) vanish, and we recover the equilibrium distribution of ions as was analyzed in Ref.[32]. In addition, Eq. (11) can also describe a steady-state situation, which differs from the equilibrium one as it allows for a non-vanishing, spatially uniform charge current density[44], as is discussed below.

Furthermore, in the limit of $\phi = 0$ and $N = 1$ (meaning $s = n$), the system contains only monovalent cations and anions. Equation (11) then reduces to the standard PNP equations

$$\begin{aligned} j_n &= -\zeta(-en\nabla\psi + k_{\mathrm{B}}T\nabla n), \\ j_p &= -\zeta(ep\nabla\psi + k_{\mathrm{B}}T\nabla p). \end{aligned} \tag{12}$$

In addition, for the fixed charge (non-CR) case, the charge density is $q = e(p-n)$, and the number density is $\rho = p+n$. Then, Eqs. (10) and (12) simplify to

$$\partial_t q = \zeta\left[k_{\mathrm{B}}T\,\nabla^2 q + \nabla\cdot(e^2\rho\nabla\psi)\right]. \tag{13}$$

We compute the product divergence in the second term of Eq. (13) and use the Poisson equation (5) for $\nabla^2\psi$. To the lowest order in the electrostatic potential with $\lambda_{\mathrm{D}}^2 = k_{\mathrm{B}}T\varepsilon/[e^2(p+n)] = k_{\mathrm{B}}T\varepsilon/(e^2\rho)$, the above equation becomes $\partial_t q = k_{\mathrm{B}}T\zeta(\nabla^2 q - \lambda_{\mathrm{D}}^{-2} q)$, which is exactly the Debye-Falkenhagen equation[43], describing the dynamics of the charge density.

Returning to the CR case, we define the density of the A^- sites combined with the total associated and dissociated B^+ particles as $\rho = s+w+p = Nn(1+\phi)+p$, and the net charge density as $q = e[p - s(1-\phi)]$. Note that ρ *should not* be confused with the local number density, $p+n$, and only in the fixed single charge (non-CR and $N=1$) case, $\rho = p+n$ as discussed above. Additionally, we define the ρ and q conjugate currents: $\mathbf{j}_\rho = \mathbf{j}_s + \mathbf{j}_w + \mathbf{j}_p$ and $\mathbf{j}_q = e(-\mathbf{j}_s + \mathbf{j}_w + \mathbf{j}_p)$.

We examine the CR effect in the steady state by setting the time derivatives in Eqs. (10)-(11) to zero and assuming spatial dependence only in the direction parallel to the external field (x-axis). This effectively reduces the problem to a one-dimensional one. To maintain a steady state, we assume that the total flux of the *number* density vanishes $j_\rho = 0$, while the net *charge* fluxes, $j_q = j_q^{\mathrm{b}}$ and $j_w = j_w^{\mathrm{b}}$, are constant. Hereafter, we use the electric field $E(x) = -\partial_x\psi$ instead of ψ, and the two ordinary differential equations for $E(x)$ and $\phi(x)$ can be derived (more details are provided in the Supplementary Material).

The boundary conditions are chosen similarly to those by Bier[44]. In the bulk, we stipulate that the electric field $E(\infty) = E_{\mathrm{b}}$, the number density $\rho(\infty) = \rho_{\mathrm{b}}$, $p(\infty) = p_{\mathrm{b}}$ and from charge neutrality, $\phi(\infty) = \phi_{\mathrm{b}} = 1 - 2p_{\mathrm{b}}/\rho_{\mathrm{b}}$. For the boundary condition at x=0, we choose $eE(0)\lambda_{\mathrm{D}}/k_{\mathrm{B}}T = 4\sigma/\sigma_{\mathrm{sat}}$, where σ is the surface charge density and $\sigma_{\mathrm{sat}} = 4\varepsilon k_{\mathrm{B}}T/(e\lambda_{\mathrm{D}})$ is the saturation charge density as defined in Ref.[45]. Note that a related steady-state case without CR effect was recently analyzed analytically in Ref.[44]; however, the CR model can only be analyzed numerically.

Thermodynamic equilibrium is characterized by $j_q^{\mathrm{b}} = 0$, as shown by the solid and dashed black lines in Fig. 2. For non-zero but constant j_q^{b}, the system deviates from equilibrium into a steady state (the solid and dashed red lines). In addition, the CR process can also be controlled through the bulk value ϕ_{b}, governed by the CR parameter α and the charge neutrality relation $\phi_{\mathrm{b}} = 1 - 2p_{\mathrm{b}}/\rho_{\mathrm{b}}$. Note that $\phi_{\mathrm{b}} = 0$ or $p_{\mathrm{b}} = \rho_{\mathrm{b}}/2$ corresponds to a constant maximum charge density on the macro-ion surface. Equivalently, it corresponds to the fixed charge (non-CR) case (dashed red and black lines). Therefore, we present four cases with the equilibrium/steady state and CR/non-CR state combinations in Fig. 2. These four schematic presentations are shown in Fig. 2(a), respectively. Figure 2(b) demonstrates that the electric field $E = -\partial_x\psi$ for the steady state decreases from its surface value to its bulk value for large x/λ_{D}. Hence, the CR process displays small differences compared to the non-CR case (solid vs. dashed red line in Fig. 2(b)).

However, a significant CR effect in the steady state is seen for both the macro-ion concentration profile $n(x)$ and the dimensionless density of the A^- sites combined with the total associated and dissociated B^+ particles $\rho(x)$, as shown in Fig. 2(c) and (e). More negatively charged macro-ions migrate towards the wall due to the electrostatic attraction, as shown in Fig. 2(c). The CR curve (red solid line) shifts significantly to the right, towards larger distances from the wall. Thus, the macro-ion density at the same distance from the wall is smaller in the CR steady state than in the equilibrium cases (solid/dashed black lines) but is larger than in the non-CR case. Additionally, as the macro-ions migrate closer to the wall, more counter-ions dissociate from their surfaces, decreasing $\phi(x)$, as shown in Fig. 2(d). This difference amounts to almost 50 % in the CR steady state.

For the non-CR case, we recall that the macro-ions trivially keep a constant charge, i.e., $\phi = 0$ (dashed red line in Fig. 2). The ρ and q plots in Fig. 2(e) and (f) follow similar tendencies as in n when comparing the four cases. In the counter-ion-only case, the distribution of the charge and particle densities are dominated by spatial dependence of macro-ions.

In the steady state, the current density of each component, denoted as $j_k, (k = s,w,p)$, has a linear dependency on the bulk value j_q^{b} as charge neutrality is obeyed. For example, for the CR case, $j_p = (p_{\mathrm{b}}/e\rho_{\mathrm{b}})j_q^{\mathrm{b}}$, and this linear dependence slope is different from that of the non-CR one, $j_p = j_q^{\mathrm{b}}/(2e)$.

While the electric current densities j_q, j_ρ, and j_p in the steady state, should be constant, it is interesting to note that each component exhibits a pronounced spatial dependence. Specifically, the charge and particle number currents j_q and j_ρ consist of four components, denoted as j_{qi} and $j_{\rho i}$, with $i = 1,2,3,4$, whereas the macro-ion current j_p contains only two components j_{p1} and j_{p2}. The four components mentioned previously correspond to different physical mechanisms driving currents. The first component is proportional to the elec-

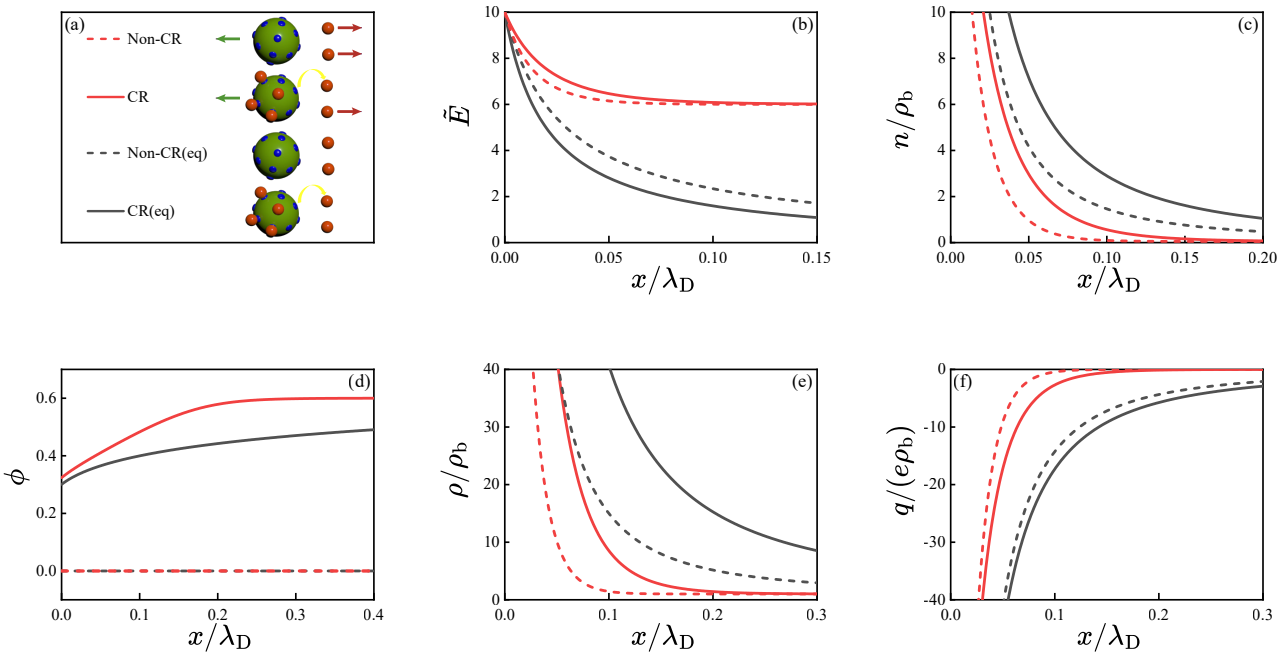

FIG. 2. (a) Schematic presentations of the four charge cases. (b) The dimensionless electric field $\tilde{E}$ (in units of $e\lambda_D/k_BT$), (c) the dimensionless macro-ion density n/ρ_b, and (d) the fraction ϕ. (e) The dimensionless density of the A^- sites combined with the total associated and dissociated B^+ particles ρ, and (f) the dimensionless charge density q/ρ_b as a function of x/λ_D, for different values of $\tilde{j}_q = j_q^b\lambda_D/(ek_BT\zeta\rho_b) = 0$ (p_b/ρ_b=0.2, CR equilibrium case, black line), $\tilde{j}_q = 0$ (p_b/ρ_b=0.5, non-CR equilibrium case, black dashed line), $\tilde{j}_q = 6$ (p_b/ρ_b=0.2, CR case, red line), and $\tilde{j}_q = 6$ (p_b/ρ_b=0.5, non-CR case, red dashed line). The other parameters are p_b/ρ_b=0.2, N=10, $\rho_b = 2\times10^{-7}$M, and σ/σ_{sat}=2.5, where $\sigma_{sat} = 4k_BT\varepsilon/(e\lambda_D)$ is the saturation charge density on the wall.

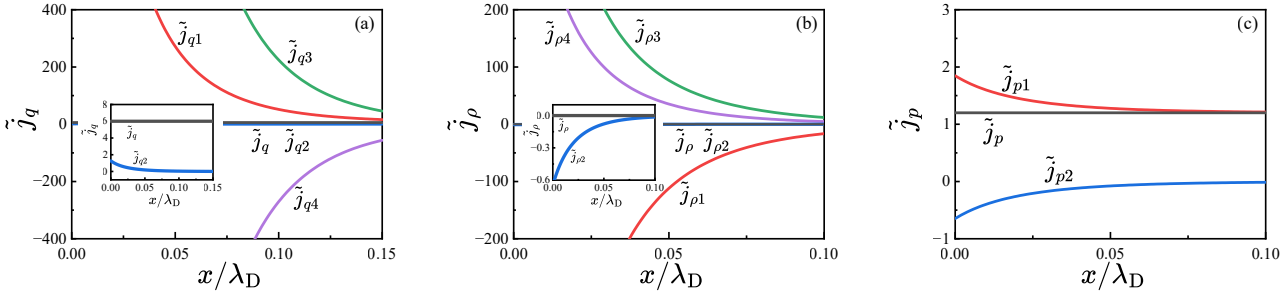

FIG. 3. (a) $\tilde{j}_q$ and its four contributions, (b) $\tilde{j}_\rho$ and its four contributions, and (c) $\tilde{j}_p$ and its two contributions, where $\tilde{j}_q$ is the current j_q rescaled by $\lambda_D/(ek_BT\zeta\rho_b)$, whereas j_ρ and j_p are rescaled by $\lambda_D/(k_BT\zeta\rho_b)$ and denoted as $\tilde{j}_\rho$ and $\tilde{j}_p$. Other parameters are $p_b/\rho_b = 0.2$, $N = 10$, $\rho_b = 2\times10^{-7}$M, $\sigma/\sigma_{sat} = 2.5$, and $\tilde{j}_q^b = 2$. The four contributions in (a) and (b) denoted as $1,...,4$ are the electric component and the three diffusive components, proportional to electrostatic field $-\partial_x\psi$ and concentration gradients $\partial_x p, \partial_x\rho$ and $\partial_x q$ respectively. Two components in (a) are proportional to $-\partial_x\psi$ and $\partial_x p$ (see Eq. (13)-(15) of the Supplementary Material). Note that the insets are added to show the variation of the curves more clearly over a smaller y-axis range.

trostatic field $E = -\partial_x\psi$. The three other components are diffusive and proportional to three concentration gradients: the free counter-ions ($\partial_x p$), the total ionic sites ($\partial_x\rho$), and the net charge ($\partial_x q$) (see Eq. (13) of the Supplementary Material for complete expressions).

The separate spatial dependence of these components is shown in Fig. 3(a), (b) and (c). Clearly, each of the components, (j_{q2}, j_{q3}, j_{q4}) and $(j_{\rho2}, j_{\rho3}, j_{\rho4})$, varies significantly as a function of the distance from the wall, despite their sum remaining constant. Additionally, the diffusive components $j_{\rho3}$ and $j_{\rho4}$, corresponding to the density of the A^- sites combined with the total associated and dissociated B^+ particles and the net charge density are significantly closer in magnitude than the j_{q3} and j_{q4}.

We have generalized Onsager's variational principle to describe the diffusive dynamics of an ionic solution containing charge-regulated (CR) macro-ions. The derived equations represent a consistent generalization of the standard PNP theory that describes fixed charge particles. By examining the steady state, we find significant CR effects on the spatial dis-

tribution of the macro-ions, particularly in the vicinity of the surface. Moreover, the electric and diffusive contributions to the current and electric charge densities have pronounced spatial variation, including a significant contribution from the CR components.

At a fixed distance from the charged surface, the macro-ion density decreases when compared with the equilibrium CR case but increases when compared to the steady-state non-CR (fixed charge) case. The CR effects, therefore, always increase the macro-ion concentration close to the boundary. In addition, the change in the number of dissociated ions from the macro-ion surface is significantly larger in the steady state compared to the equilibrium one, implying that the CR effect strengthens in the non-equilibrium steady state. In the steady state, the macro-ions' distribution is more compressed. It shifts closer to the charged wall, as shown in Fig. 2(c). This compression results from the steady-state current. Unlike the pure electrostatic mechanism in equilibrium systems, the CR effect in NESS differs from its equilibrium counterpart due to the coupling with the ionic diffusive dynamics. These findings indicate that the CR effect is more pronounced in experiments under non-equilibrium conditions. For example, it affects the charge of proteins as they move in cellular environments, affecting their adsorption or binding affinity to membranes. Likewise, it influences the stability of charged nanoparticle suspensions.

This study employs four assumptions. (i) We assume that the Poisson equation also holds for the slow dynamics considered here, implying that the electrostatic potential is a fast dynamical variable and is always equilibrated. (ii) The CR process is coupled only to the ionic diffusive dynamics. (iii) The charged wall maintains a constant surface charge density, serving as a boundary condition. We focus on the diffusive process occurring in the intermediate spatial region, which is neither close to nor far from the wall. This agrees with experimental situations where the current has not yet neutralized the charged wall. Hence, we ignore the current absorption kinetics at the wall. (V) We utilize the OVP approach within the mean-field description. This limits the model to cases where fluctuations are small, and the electrolyte solution is dilute and weakly charged. Our theory offers a unified and consistent way to deal with CR diffusive dynamics for systems undergoing charge association/dissociation processes with the bathing solution. Our results, along with the generalization of Onsagers variational principle, provide insights into understanding diverse experimental systems that involve charge regulation mechanisms. These systems encompass the electrophoresis of DNA/RNA in microfluidic channels, as well as the transport of biomolecules, such as proteins and other components of living matter.

ACKNOWLEDGMENTS

We thank M. Doi for his helpful comments and discussions. BZ thanks F. F. Ye for the support on computing resources and acknowledges the National Natural Science Foundation of China (NSFC) through Grants No. 22203022 and the Scientific Research Starting Foundation of Wenzhou Institute, UCAS (No. WIUCASQD2022016). SK acknowledges the NSFC through Grants Nos. 12274098 and 12250710127 and the startup fund of Wenzhou Institute, UCAS (No. WIUCASQD2021041). DA acknowledges the NSFC-ISF Research Program, jointly funded by the NSFC under grant No. 21961142020 and the Israel Science Foundation (ISF) under grants No. 3396/19 and ISF grant No. 226/24. RP acknowledges funding from the NSFC Key Project No. 12034019.

DATA AVAILABILITY STATEMENT

The data that supports the findings of this study are available within the article [and its Supplementary Material].

SUPPLEMENTARY MATERIALS

Detailed derivation for equations in the steady state and the list of variables in this work.

REFERENCES

[1] M. Lund and B. Jönsson, "Charge regulation in biomolecular solution," Q. Rev. Biophys. **46**, 265–281 (2013).
[2] T. Markovich, D. Andelman and R. Podgornik, "Charged membranes: PoissonBoltzmann theory, the DLVO paradigm, and beyond," In Handbook of lipid membranes, CRC Press, pp 99–128 (2021).
[3] Y. Avni, D. Andelman and R. Podgornik, "Charge regulation with fixed and mobile charged macromolecules," Curr. Opin. Electrochem. **13**, 70–77 (2019).
[4] H. X. Zhou and X. Pang, "Electrostatic interactions in protein structure, folding, binding, and condensation," Chem. Rev. **118**, 1691–1741 (2018).
[5] A. Boi and R. Podgornik, "Site correlations, capacitance, and polarizability from protein protonation fluctuations," J. Phys. Chem. B **125**, 12902–12908 (2021).
[6] G. M. Ong, A. Gallegos and J. Wu, "Modeling surface charge regulation of colloidal particles in aqueous solutions," Langmuir **36**, 11918–11928 (2020).
[7] M. Borkovec, B. Jönsson and G. J. Koper, "Ionization processes and proton binding in polyprotic systems: small molecules, proteins, interfaces, and polyelectrolytes," In Surface and Colloid Science, Springer, pp 99–339 (2001).
[8] I. Borukhov, D. Andelman, R. Borrega, M. Cloitre, L. Leibler and H. Orland, "Polyelectrolyte titration: theory and experiment," J. Phys. Chem. B **104**, 11027–11034 (2000).
[9] G. L. Celora, R. Blossey, A. Münch and B. Wagner, "Counterion-controlled phase equilibria in a charge-regulated polymer solution," J. Chem. Phys. **159**, 184902 (2023).
[10] F. L. B. da Silva, P. Derreumaux and S. Pasquali, "Protein-RNA complexation driven by the charge regulation mechanism," Biochem. Biophys. Res. Commun. **498**, 264–273 (2018).
[11] B. Zheng, Y. Avni, D. Andelman and R. Podgornik, "Phase separation of polyelectrolytes: the effect of charge regulation," J. Phys. Chem. B **125**, 7863–7870 (2021).
[12] K. Hyltegren and M. Skepö, "Adsorption of polyelectrolyte-like proteins to silica surfaces and the impact of pH on the response to ionic strength. a Monte Carlo simulation and ellipsometry study," J. Colloid Interface Sci. **494**, 266–273 (2017).
[13] T. Obstbaum and U. Sivan, "Thermodynamics of charge regulation near surface neutrality," Langmuir **38**, 8477–8483 (2022).

[14] Y. Hong and D. G. Brown, "Electrostatic behavior of the charge-regulated bacterial cell surface," Langmuir **24**, 5003–5009 (2008).
[15] R. J. Nap, A. L. Božič, I. Szleifer and R. Podgornik, "The role of solution conditions in the bacteriophage PP7 capsid charge regulation," Biophys. J. **107**, 1970–1979 (2014).
[16] G. M. Ong, A. Gallegos and J. Wu, "Modeling surface charge regulation of colloidal particles in aqueous solutions," Langmuir **36**, 11918–11928 (2020).
[17] J. Yuan, K. Takae and H. Tanaka, "Impact of charge regulation on self-assembly of zwitterionic nanoparticles," Phys. Rev. Lett. **128**, 158001 (2022).
[18] B.W. Ninham and V. A. Parsegian, "Electrostatic potential between surfaces bearing ionizable groups in ionic equilibrium with physiologic saline solution," J. Theor. Biol. **31**, 405–428 (1971).
[19] H. Diamant and D. Andelman, "Kinetics of surfactant adsorption at fluid-fluid interfaces," J. Phys. Chem. **100**, 13732–13742 (1996).
[20] B. Werkhoven, S. Samin and R. van Roij, "Dynamic stern layers in charge-regulating electrokinetic systems: three regimes from an analytical approach," Eur. Phys. J.: Spec. Top. **227**, 2539–2557 (2019).
[21] J. C.Everts, S. Samin, N. A. Elbers, J. E. S. van der Hoeven, A. van Blaaderen and R. van Roij, "Colloidoilwater-interface interactions in the presence of multiple salts: charge regulation and dynamics," Phys. Chem. Chem. Phys. **19**, 14345–14357 (2017).
[22] D. Sean, J. Landsgesell and C. Holm, "Influence of weak groups on polyelectrolyte mobilities," Electrophoresis **40**, 799-809 (2019).
[23] J. X. Yuan, T. Curk, "Collapse/expansion dynamics and actuation of pH-responsive nanogels," arXiv:2405.19193 (2024).
[24] P. Biesheuvel and M. Bazant, "Analysis of ionic conductance of carbon nanotubes," Phys. Rev. E **94**, 050601 (2016).
[25] Z. Jiang and D. Stein, "Charge regulation in nanopore ionic field-effect transistors," Phys. Rev. E **83**, 031203 (2011).
[26] C. L. Ritt, J. P. de Souza, M. G. Barsukov, S. Yosinski, M. Z. Bazant, M. A. Reed and M. Elimelech, "Thermodynamics of charge regulation during ion transport through silica nanochannels," ACS Nano **16**, 15249–15260 (2022).
[27] M. Z. Bazant, M. S. Kilic, B. D. Storey and A. Ajdari, "Towards an understanding of induced-charge electrokinetics at large applied voltages in concentrated solutions," Adv. Colloid Interface Sci. **152**, 48–88 (2009).
[28] M. S. Kilic, M. Z. Bazant, and A. Ajdari, "Steric Effects in the dynamics of electrolytes at large applied voltages. II. modified Poisson-Nernst-Planck equations," Phys. Rev. E **75**, 021503 (2007).
[29] Y. Avni, T. Markovich, R. Podgornik and D. Andelman, "Charge regulating macro-ions in salt solutions: screening properties and electrostatic interactions," Soft Matter **14**, 6058–6069 (2018).
[30] Y. Avni, R. Podgornik and D. Andelman, "Critical behavior of charge-regulated macro-ions," J. Chem. Phys. **153**, 024901 (2020).
[31] R. Podgornik, "General theory of charge regulation and surface differential capacitance," J. Chem. Phys. **149**, 104701 (2018).
[32] T. Markovich, D. Andelman and R. Podgornik, "Complex fluids with mobile charge regulating macro-ions," EPL **120**, 26001 (2018).
[33] M. Doi, "Soft Matter Physics," (Oxford University Press, Oxford, 2013).
[34] M. Doi, "Onsagers variational principle in soft matter," J. Phys.: Condens. Matter **23**, 284118 (2011).
[35] M. Doi, "Onsager principle in polymer dynamics," Prog. Polym. Sci. **112**, 101339 (2021).
[36] M. Arroyo, N. Walani, A. Torres-Sánchez and D. Kaurin, "Onsagers variational principle in soft matter: introduction and application to the dynamics of adsorption of proteins onto fluid membranes," In The role of mechanics in the study of lipid bilayers, Springer, pp 287–332 (2018).
[37] H. Wang, T. Qian and X. Xu, "Onsager's Variational principle in active soft matter," Soft Matter **17**, 3634–3653 (2021).
[38] L.-S. Lin, K. Yasuda, K. Ishimoto, Y. Hosaka and S. Komura, "Onsagers variational principle for nonreciprocal systems with odd elasticity," J. Phys. Soc. Jpn. **92**, 033001 (2023).
[39] S. Xu, R. Eisenberg, Z. Song and H. Huang, "Coupled chemical reactions: effects of electric field, diffusion, and boundary control," Phys. Rev. E **108**, 064413 (2023).
[40] J. Gu and P. Gaspard, "Stochastic approach and fluctuation theorem for charge transport in diodes," Phys. Rev. E **97**, 052138 (2018).
[41] M. Z. Bazant, "Theory of chemical kinetics and charge transfer based on nonequilibrium thermodynamics," Acc. Chem. Res. **46**, 1144–1160 (2013).
[42] N. Gavish, D. Elad and A. Yochelis, "From solvent-free to dilute electrolytes: essential components for a continuum theory," J. Phys. Chem. Lett. **9**, 36–42 (2018).
[43] M. Janssen and M. Bier, "Transient dynamics of electric double-layer capacitors: exact expressions within the Debye-Falkenhagen approximation," Phys. Rev. E **97**, 052616 (2018).
[44] M. Bier, "Non-equilibrium steady states of electrolyte interfaces," New J. Phys. **26**, 013008 (2024)
[45] M. V. Fedorov and A. A. Kornyshev, "Towards understanding the structure and capacitance of electrical double layer in ionic liquids," Electrochimica Acta **53**, 6835–6840 (2008).